JVI Accepts, published online ahead of print on 3 October 2012
J. Virol. doi:10.1128/JVI.01973-12

Acid-activated structural reorganization of the Rift Valley fever virus Gc fusion protein

S.M. de Boer[a,b], J. Kortekaas[b], L. Spel[a], P.J.M. Rottier[a], R.J.M. Moormann[a,b], B.J. Bosch[a]#

a Department of Infectious Diseases and Immunology, Virology Division, Faculty of Veterinary Medicine, Utrecht University, Yalelaan 1, 3584 CL, Utrecht, The Netherlands

b Central Veterinary Institute of Wageningen University and Research Centre, Department of Virology, Edelhertweg 15, 8219 PH, Lelystad, The Netherlands

Corresponding author: b.j.bosch@uu.nl

Abstract

Entry of the enveloped Rift Valley fever virus (RVFV) into its host cell is mediated by the viral glycoproteins Gn and Gc. We investigated the RVFV entry process and its pH-dependent activation mechanism in particular using our recently developed nonspreading RVFV particle system. Entry of the virus into the host cell was efficiently inhibited by lysosomotropic agents that prevent endosomal acidification and by compounds that interfere with dynamin- and clathrin-dependent endocytosis. Exposure of plasma membrane-bound virions to an acidic pH (<pH 6) equivalent to the pH of late endo-lysosomal compartments allowed the virus to bypass the endosomal route of infection. Acid exposure of virions in the absence of target membranes triggered the class II-like Gc fusion protein to form extremely stable oligomers, resistant to SDS- and temperature-dissociation, and concomitantly compromised virus infectivity. By targeted mutagenesis of conserved histidines in Gn and Gc, we demonstrate that mutation of a single histidine (H857) in Gc completely abrogates virus entry as well as acid-induced Gc oligomerization. In conclusion, our data suggest that after endocytic uptake, RVFV traffics to the acidic late endo-lysosomal compartments where histidine protonation drives the reorganization of the Gc fusion protein that leads to membrane fusion.

Introduction

Rift Valley fever virus (RVFV) is an emerging pathogen that affects ruminants and humans and is transmitted between susceptible hosts by different species of mosquitoes. RVFV was first isolated in Kenya in 1930, and has since spread throughout the African continent and the Arabian Peninsula (12, 46). An outbreak of RVFV can have a devastating socio-economic impact on the region (2, 18, 50) and is characterized by abortion storms in adult livestock and high mortality among newborns. Humans can also be infected through contact with infected tissues or via mosquito bites, typically causing a self-limiting febrile illness. A small percentage of human infections result in hemorrhagic fever or encephalitis with generally fatal outcome (41).

RVFV belongs to the *Phlebovirus* genus of the *Bunyaviridae* family, which comprises four additional genera (*Orthobunyavirus, Hantavirus, Nairovirus and Tospovirus*). Members of the *Bunyaviridae* family are enveloped viruses of ~100 nm in size that have a tripartite negative-strand RNA genome which is replicated in the cytoplasm. The genomic segments are encapsidated by the nucleocapsid protein forming the ribonucleoproteins (RNPs) (56). The lipid envelope surrounding the RNPs contains an ordered shell made up by units of two glycoproteins, Gn and Gc (20). These glycoproteins are responsible for entry into the host cell but their precise functional roles in receptor binding and fusion are poorly understood. Gn and Gc are type-I membrane glycoproteins which form heterodimers after post-translational processing of a glycoprotein precursor in the endoplasmic reticulum. By virtue of a Golgi-localization signal in Gn, the Gn-Gc heterodimers are targeted to the Golgi apparatus (56, 65). Here, interaction between the Gn carboxyl-terminal cytoplasmic tail and the RNPs allows virus budding into the lumen of the Golgi-cisternae (45, 47, 56). In the case of the RVFV virion, a 78-kDa protein consisting of pre-Gn and Gn regions has been identified as a third but minor structural component (27, 60). Cryo-electron microscopy studies of RVFV virions showed that the viral envelope comprises 720 heterodimers of Gn (54-kDa) and Gc (56-kDa), forming 110 cylinder-shaped hexamers and 12 pentamers according to a T=12 icosahedral lattice (13, 24).

Enveloped viruses carry dedicated proteins in their envelope which mediate fusion between viral and cellular membranes allowing translocation of the viral genome into the cytoplasm. This membrane fusion process is driven by structural rearrangements in the metastable viral fusion protein which are triggered by either receptor binding, proteolytic cleavage or the acidic pH of endosomes allowing fusion to occur at the right time and place (8). Viral fusion proteins have been divided into three

classes (class I, II and III) based on their structural features (67). The Gc glycoprotein of bunyaviruses has been proposed to be a class II viral fusion protein (15, 53). Similar to class II fusion proteins of alphaviruses and flaviviruses, Gc is predicted to be mainly composed of β-sheet structures, is synthesized from a polyprotein downstream of a companion protein (Gn) and assembles into a heterodimer in the ER (15, 48, 62, 63).

Common to all class II fusion proteins is that they utilize the low pH in the acidified endosome to activate their fusion process. Low pH triggers the dissociation of the glycoprotein dimeric state, resulting in exposure and subsequent insertion of a highly hydrophobic stretch of amino acids. Insertion of this fusion peptide into the target membrane is followed by trimerization of the monomeric fusion proteins. A stable trimeric hairpin structure is subsequently formed which brings together the fusion peptide and transmembrane domain at one end of the molecule, mediating the fusion of the cellular and viral membrane. While the acid-induced conformational changes of class II viral fusion proteins have been well documented (see for an comprehensive review (30)), the mechanism of low pH triggering is not well understood. Protonation of histidines has been suggested to act as a molecular switch that triggers the activity of pH-activated viral fusion proteins (4, 28). The rationale for this hypothesis is that histidine is the only amino acid residue with a side-chain pKa value (pKa 6.4) within the pH range found in the endo-lysosomal pathway (pH 4.5-6.5) (28, 54). Evidence in support of a crucial role for histidine protonation in promoting fusion protein rearrangements leading to fusion has been obtained for a number of low pH-dependent viruses (3, 4, 6, 14, 26, 34, 36, 49, 57, 61).

Knowledge on the fusion mechanism of bunyaviruses is still in its infancy. In agreement with a class II virus classification, bunyaviruses appear to have an acid-dependent fusion machinery. Exposure of cells overexpressing RVFV Gn and Gc to low pH results in the formation of multi-nucleated cells (11). Acid-induced syncytia formation has also been reported for other members of the *Bunyaviridae* family including Uukuniemi virus (UUKV, *Phlebovirus* genus), La Crosse virus (*Orthobunyavirus* genus) and Hantaan virus (*Hantavirus* genus) (1, 39, 42, 48). In accordance with the hypothesis of acid-induced fusion activation, bunyaviruses are sensitive to acidotropic agents which raise the pH of intracellular endocytic compartments (55, 58). In addition, acid-exposure of plasma membrane-bound UUKV could bypass the endosomal acidic pH requirement, needed for infection (39).

In this study we have examined the entry mechanism of RVFV. Studies on natural RVFV strains have been hampered by the requirement of handling the virus under biosafety level-3 containment (BSL-3).

We have taken advantage of our recently established nonspreading RVFV ($RVFV_{ns}$) production system which can be handled outside of BSL-3 (33). This system allows the efficient production of RVFV particles upon transfection of a single Gn/Gc-expression plasmid into a replicon cell line which maintains the replication machinery of RVFV. The expression of the eGFP gene from the viral genome enables infection to be easily monitored. Most importantly, the system greatly facilitates Gn and Gc structure/function studies as long as particle assembly is not compromised. Using $RVFV_{ns}$, we have examined the endocytic uptake of the virus, the low pH dependence and kinetics of virus entry, the effects of low pH treatment of the virus on infectivity and rearrangement of the glycoproteins as well as the role of conserved histidines in Gn and Gc in virus entry.

Material and methods

Cells and viruses

BHK cells were grown in Glasgow minimum essential medium (GMEM; Invitrogen) supplemented with 4% tryptose phosphate broth, 1% minimum essential medium nonessential amino acids (MEM NEAA; Invitrogen), and 5% (v/v) fetal calf serum (FCS; Bodinco). For maintenance of BHK-Rep2 cells (33), Geneticin (G-418) was used at a concentration of 1 mg/ml. A549 and CHO K1 cells were grown in Dulbecco's Modified Eagle Media (DMEM; Lonza, Biowhittaker) and Ham's F-12K medium (Invitrogen), respectively, supplemented with 10% FCS. Cells were grown at 37°C and 5% CO_2. Drosophila Schneider (S2) cells (Invitrogen) were grown at 27°C in serum-free InsectXpress medium (Lonza). Recombinant RVFV ($RVFV_{rec}$) and $RVFV_{ns}$ have both been rescued from cDNA as described (33). VSV-ΔG/GFP/G* is a recombinant vesicular stomatitis virus of which the glycoprotein gene has been replaced by that of GFP. The virus was pseudotyped with its authentic glycoprotein G as described (5).

Plasmids

The QuickChange XL site-directed mutagenesis kit (Stratagene) was used to exchange specific histidine for alanine codons in the pCAGGS-M expression plasmid (33) according to the manufacturer's protocol at amino acid positions 157, 540, 572, 580, 778, 836, 857, 1087 of the RVFV M segment (GenBank:JF784387). The recombinant plasmids were sequenced to confirm that only the desired mutations were present.

To generate a stable *Drosophila* S2 cell line expressing the Gc ectodomain (Gce) of RVFV (GenBank:JF784387), a truncated version of the Gn-Gc coding sequence lacking the transmembrane and cytoplasmic domain of Gc (GnGce; 153-AEDPHL / FGGPLK-1158) was cloned into the pMT/BiP/V5-HisA (Invitrogen) expression vector downstream of the BiP encoding signal sequence. A quadruple Strep-tag encoding sequence separated by glycine linkers ($(DPTGWSHPQFEK(GGGSGGGSGGGSWSHPQFEK)^3$) was appended C-terminally to allow purification of the secreted Gc ectodomain from the culture supernatant using Strep-Tactin sepharose

affinity chromatography (IBA GmbH). Stable S2 cell lines were generated according to the manufacturer's protocol (Invitrogen) with minor modifications. S2 cells were transfected with the expression vector and pCoBlast plasmid in a 1:19 ratio. Stable cell lines were subsequently selected at 27°C in serum-free InsectXpress medium containing 25 µg/ml Blasticidin-S-HCl (Invitrogen) and maintained in this culture medium in the presence of 10 µg/ml Blasticidin-S-HCl.

Production of polyclonal antiserum against Gc ectodomain

Polyclonal antibodies were raised against Gc-ectodomain after immunization of rabbits (Davids biotechnologie). Rabbits were immunized at day 0, 14 and 21 with ~40 µg of Strep-tag purified Gc-ectodomain. Total serum was collected at day 35.

Chemicals

Bafilomycin A1, dynasore, cytochalasin D, nystatin (Sigma) and dyngo-4a (Abcam) were prepared in dimethylsulfoxide (DMSO). Chlorpromazine and ammonium chloride (Sigma) were prepared in distilled sterile water. Diethyl pyrocarbonate (DEPC, Sigma) was dissolved in 96% ethanol.

Fluorescence-activated cell sorting (FACS)

Flow cytometry was performed on a FACS Calibur flow cytometer (Becton Dickinson Immunocytometry Systems). For the analysis of the data, Cyflogic 1.2.1 software was used.

Fluorescence microscopy

Fluorescence microscopy on living or fixed cells (fixed with 3.7% formaldehyde for 20 minutes at room temperature) was performed on the EVOS fl microscope (AMG). Nuclei of fixated cells were stained with 4'-6-diamidino-2-phenylindole (DAPI).

Production of RVFV$_{ns}$ particles

RVFV$_{ns}$ particles were produced as described (33). In short, BHK-rep2 cells (33) were seeded in Optimem medium (Invitrogen) supplemented with 2% FCS. Cells were transfected (JetPEI, Polyplus) with pCAGGS-M (or derivatives thereof) in Optimem containing 0.2% FCS. Twenty hours post transfection the RVFV$_{ns}$ particles in the collected medium were concentrated and transferred into a phosphate buffered saline (PBS) or HNE pH 7.4 buffer (5mM HEPES, 150mM NaCl, 0.1mM EDTA) using Amicon® Ultra centrifugal filters (Millipore) with a molecular weight cut-off of 100,000 kilodalton (Millipore). Titers of RVFV$_{ns}$ stocks were determined by TCID$_{50}$ analysis as described (33).

Inhibition of RVFV infection by pharmacological drugs

To analyze the effects of specific drugs on RVFV entry, BHK-21 cells were pre-treated for one hour with ammonium chloride, chlorpromazine (both dissolved in water), bafilomycin A1, cytochalasin D, dynasore, dyngo-4a or nystatin (the latter four dissolved in DMSO). Cells were inoculated for two hours with RVFV$_{ns}$ or VSV$_{ns}$ (moi ~0.4) at 37°C, before the culture medium was replaced by medium containing 10 or 40 nM bafilomycin A1, respectively. Cells were further incubated at 37°C. Inhibitory effects of the compounds on virus replication were tested by addition of the chemicals two hours post infection (hpi). After a period of three hours the drug containing medium was replaced by culture medium containing bafilomycin (10 nM). RVFV$_{ns}$ or VSV$_{ns}$ infection was quantified at 20 or 8 hours after virus inoculation, respectively, by analysis of GFP-expressing cells using FACS or fluorescence microscopy. Viability of the drug-treated cells was measured using a WST-1 assay (Roche) according to manufacturers' recommendations.

Ammonium chloride add-in time course

Infection was synchronized by allowing RVFV$_{ns}$ particles to bind to cells on ice for 1 h in serum free medium. The cells were washed with cold medium to remove unbound virus and subsequently transferred rapidly to a 37°C water bath after addition of serum free pre-warmed Roswell Park Memorial Institute 1640 medium (RPMI-1640, Invitrogen) adjusted at different pHs. Ammonium chloride (10 mM) was added to the medium at indicated times. Infection (GFP-positive cells) was quantified at 18 hours post warming by FACS and fluorescence microscopy.

193

194 **Polyacrylamide gel electrophoresis (PAGE), Western blotting and dot-blot analysis**

195 Samples containing $RVFV_{ns}$ particles were heated for 10 minutes at 40-80°C in Laemmli sample buffer
196 lacking β-mercaptoethanol (LSB-) and loaded onto NuPAGE® bis-tris gels (Invitrogen). After
197 separation, proteins were blotted onto polyvinylidene fluoride (PVDF) membranes. Western blot
198 analysis was performed using a rabbit Gc peptide antiserum (9), a rabbit polyclonal serum against Gce
199 (see above), the 4-D4 mouse αGn monoclonal antibody (provided by Dr. Connie Schmaljohn,
200 USAMRIID) (29) or a sheep polyclonal antiserum against RVFV (32) as the primary antibody and an
201 appropriate peroxidase-conjugated secondary antibody. For dot blot analysis, samples containing
202 $RVFV_{ns}$ particles were heated for 20 minutes at 80°C and spotted onto nitrocellulose membrane
203 (Whatmann). The membrane was blocked with PBS containing 0,05% Tween20 (v/v) and 5% protifar
204 (w/v, Nutricia). $RVFV_{ns}$ particles were detected using the 4-D4 αGn monoclonal antibody.

205

206 **Fusion at the plasma membrane**

207 $RVFV_{ns}$ particles were allowed to bind to a confluent layer of BHK-21 cells on ice for 2 hours. Cell-
208 bound virus was subsequently exposed to pre-warmed RPMI-1640 medium for 3 minutes at 37°C
209 (water bath). The pH of the culture medium varied from pH 7.4 to 5.0. The RPMI medium was
210 replaced by culture medium containing bafilomycin A1 (20nM) and cells were further incubated at
211 37°C, 5% CO_2. Twenty hours after the 3 minute pH-shock, infection (GFP-positive cells) was
212 quantified by FACS and fluorescence microscopy.

213

214 **Low pH treatment of $RVFV_{ns}$ particles**

215 $RVFV_{ns}$ particles in HNE buffer pH 7.4 were exposed to conditions ranging from pH 7.4 to 5.0 by
216 addition of a pre-titrated volume of 100mM MES (pH 6.5 to 5.3) or 200mM HAc (pH 5.0). The particles
217 were incubated for 3 minutes at the desired pH at 37°C before the samples were back-neutralized to
218 pH 7.4 with 0.1N NaOH. Samples were subsequently used to infect BHK-21 cells and infection was
219 analyzed 20 hpi by FACS and fluorescence microscopy. To analyze the effect of low pH treatment on
220 the structural glycoproteins Gn and Gc, the pH of HNE buffered $RVFV_{ns}$ particles was varied from pH

7.4 to 4.25 by addition of MES (pH 6.5 to 5.3), 200mM HAc (pH 5.0 to 4.75) or 500mM HAc (pH 4.5 to 4.25). The $RVFV_{ns}$ particles were incubated for 0-10 minutes at 37°C and the buffer was subsequently returned to pH 7.4 by adding a predetermined amount of 0.1N NaOH or 0.5N NaOH (pH 4.25). Samples were analyzed by Western blotting as described.

DEPC treatment of $RVFV_{ns}$ particles

A diethylpyrocarbonate (DEPC) solution (1M) in 96% ethanol was freshly prepared from a 1.12 g/ml commercial stock (Sigma). $RVFV_{ns}$ particles in PBS were incubated with indicated concentrations of DEPC for 10 minutes at 37°C. BHK-21 cells were inoculated with the treated virus for 20 hours and assayed for infection (GFP-positive cells) by FACS and fluorescence microscopy.

Statistics

The data are representative of multiple independent experiments. Values are shown as mean values ± standard deviation (SD). Standard deviations were calculated using GraphPad Prism version 5.00 for Windows (GraphPad Software).

Results

Entry of RVFV by endocytic uptake

We started our studies on RVFV cell entry with a limited pharmacological drug screen to investigate the uptake of the virus into cells using established inhibitors of cellular endocytic pathways. BHK-21 cells were pre-treated for one hour with different concentrations of drugs that interfere with dynamin-2 (dynasore), caveolin- (nystatin), clathrin- (chlorpromazine) or actin- (cytochalasin D) dependent endocytosis. Cells were then inoculated with nonspreading RVFV ($RVFV_{ns}$) at a moi of ~0.4 in the presence of the drugs and subsequently incubated without the drugs but in the presence of bafilomycin A1 to inhibit further infection (Fig. 1A). A nonspreading recombinant of VSV (VSVΔG-GFP/G*, in short VSV_{ns}) was taken along as a control virus (5). Both viruses express GFP from the viral genome facilitating quantification of infection. Treatment of BHK-21 cells with dynasore or chlorpromazine, but not with the other compounds tested, reduced RVFV infection considerably, stronger even than they affected VSV infection, which is well known to be dependent on dynamin-2 and clathrin during entry (Fig. 1A). The presence of these drugs did not have a significant effect on the cell viability (Fig. 1B). Importantly, infection of $RVFV_{ns}$ was hardly affected if dynasore or chlorpromazine was added two hours post inoculation, indicating that the drugs only affect the entry stage of infection (Fig 1C). Similar effects of dynasore and chlorpromazine on $RVFV_{ns}$ infection were seen on A549 cells (data not shown). We confirmed the involvement of dynamin-2 in $RVFV_{ns}$ entry on BHK-21 cells using a novel and potent inhibitor of dynamin-2 named dyngo-4a (23) (Fig. 1B and Fig. 1D). Dynasore and chlorpromazine also strongly inhibited entry of a recombinant $RVFV_{rec}$ expressing GFP (Fig 1E). These drug inhibition data indicate that entry of RVFV is sensitive to inhibitors which interfere with dynamin-2 and clathrin-dependent endocytosis.

RVFV entry depends on vacuolar acidification

Previously it was described that low pH incubation of cells overexpressing the RVFV glycoproteins resulted in extensive cell-cell fusion, suggesting that after endocytosis RVFV fusion is activated by the acidic environment of endosomal compartments (11, 37). To explore the requirements of a low endosomal pH for virus entry we analyzed the infection of $RVFV_{ns}$ in the presence of the

lysosomotropic agents bafilomycin A1, an inhibitor of vacuolar-type H+-ATPase proton pumps, and the lipophilic weak base ammonium chloride (NH_4Cl), which both prevent acidification of endosomal compartments. VSV_{ns}, known to be acid-activated in early endosomes with a pH threshold of pH 6.1 (35, 68), was used as a control. The results demonstrate that $RVFV_{ns}$ entry is strictly dependent on vacuolar acidification as infection of BHK-21 and A549 cells was inhibited by bafilomycin A1 as well as by NH_4Cl (Fig. 2A). Compared to VSV_{ns}, $RVFV_{ns}$ appears to be more sensitive to the lysosomotropic agents suggesting that the virus has a lower pH threshold for activation and therefore may be activated in more acidic vacuoles beyond the early endosomal compartments.

To define the time of acid exposure after receptor binding we used a previously described NH_4Cl add-in experiment (40). Addition of NH_4Cl to the medium is known to almost instantly raise the endosomal pH (43) allowing studies on the kinetics by which viruses pass the acid-requiring entry step after binding. We synchronized the infection of $RVFV_{ns}$ by allowing the virus to bind to cells in the cold. After removal of the unbound virus, we rapidly transferred the cells to 37°C and added 10mM NH_4Cl at different times post warming. About ninety percent of the virus experienced the acid-requiring step between 4 to 48 minutes after warming of the cells (Fig. 2B). The entry kinetics of $RVFV_{ns}$ are similar to those reported for the *Phlebovirus* UUKV (39) and influenza viruses (40), which were both shown to fuse at low pH in late endosomal or lysosomal compartments (38, 39, 69).

RVFV fusion occurs at acidic conditions that resemble the endo-lysosomal compartments

To determine the pH threshold for fusion of RVFV we measured infection after low-pH induced fusion at the plasma membrane under conditions where acidification of endosomes - and normal virus entry - is blocked by bafilomycin A1. In this acid-mediated endocytosis bypass experiment, that was previously described for SFV and UUKV (19, 39), $RVFV_{ns}$ particles were bound to cells in the cold and subsequently exposed for 3 minutes at 37˚C to media with varying pH. Medium was replaced with culture medium containing bafilomycin A1 to inhibit further infection via the endocytic pathway. The results demonstrate that treatment of the cell-bound virus at or below pH 5.5 fully bypassed the requirement for vacuolar acidification (Fig. 3A). The bypass was less efficient at pH 5.7 and only limited infection was observed at pH 6 or higher, indicating that the pH threshold for RVFV membrane fusion is around pH 5.7. Exposure of free $RVFV_{ns}$ particles to low pH (pH 6.5 - 5) for 3 minutes did reduce virus infectivity, although virus inactivation was not complete (Fig. 3B).

296

297 **Acid induced rearrangement of the Gc into higher-order structures**

298 Next we examined the effects of exposure to low pH on the structural organization of the RVFV
299 envelope glycoproteins. $RVFV_{ns}$ particles were incubated in buffers of low pH for 10 minutes. After
300 neutralization of the buffers, viral proteins were analyzed by Western blotting performed under non-
301 reducing conditions. The Gn and Gc glycoproteins as well as the 78-kDa protein were detected using
302 a polyclonal RVFV serum, a Gn-specific monoclonal antibody and with a Gc-specific peptide serum
303 (Fig. 4A). Incubation of $RVFV_{ns}$ at the low pH conditions that activate virus entry (pH<6; Fig. 3A) led to
304 the disappearance of the Gc monomer and the concomitant appearance of a more slowly migrating
305 protein moiety. Incubation at low pH did not influence migration of the Gn or the 78k-Da protein. The
306 disappearance of the Gc monomer suggested that the slowly migrating band consists of an oligomer
307 of Gc, which can be detected by the polyclonal RVFV serum but, perhaps through epitope
308 inaccessibility, not by the Gc peptide serum. Consistent with this notion, heating of acid-activated
309 $RVFV_{ns}$ to 90°C resulted in the disappearance of the slowly migrating band and the simultaneous
310 appearance of monomeric Gc (Fig. 4B). To further study the identity of the presumed Gc oligomer we
311 produced a polyclonal antiserum by inoculating rabbits with the ectodomain of Gc produced using the
312 *Drosophila* expression system. This antiserum efficiently recognized the monomeric as well as the
313 slower migrating form of Gc on Western blots confirming the identity of the Gc oligomer (Fig. 4C).
314 Using this antiserum, we analyzed the kinetics of Gc oligomer formation. The conversion of Gc into
315 SDS-stable oligomers slowly increased with time of pH treatment (Fig. 4C). Conversion became
316 detectable already after 15 seconds and was nearly complete after 4 minutes of incubation at low pH.
317 These results demonstrate that incubation of RVFV at the fusion-activating pH triggers a structural
318 reorganization of Gc from an apparently metastable to a highly stable oligomeric conformation,
319 reminiscent of the stable acid-activated trimeric class II fusion proteins of alpha- and flaviviruses (31,
320 59, 64).

321

322 **RVFV entry is inhibited by substitution of a single histidine in Gc**

323 Protonation of one or more histidines can be crucial for triggering conformational changes in viral
324 fusion proteins (28). A first clue for a ´pH sensing´ role of histidines in RVFV infection came from the

observation that pre-incubation of $RVFV_{ns}$ with diethylpyrocarbonate (DEPC), a chemical which specifically modifies the aromatic ring of histidines preventing its protonation (7), clearly inhibits RVFV infection of BHK-21 cells in a concentration dependent manner (Fig. 5A). To further study the role of histidine protonation in entry, we identified and replaced eight conserved histidines in Gn and Gc (Table 1 and Fig. 5B) by the small and non-polar amino acid alanine. $RVFV_{ns}$ particles carrying the histidine-to-alanine replacements were produced and secreted from BHK-21 replicon cells (33) with efficiencies resembling that of wild-type $RVFV_{ns}$, indicating that the mutations in Gn and Gc did not impair assembly and release of virus particles (data not shown). Amounts of mutant and wildtype virus particles were normalized using a dot blot assay and equal virus quantities were compared for their relative infectivity's (Fig. 5C). $RVFV_{ns}$ mutants with histidine-to-alanine substitutions in Gn were all viable although their infectivity was slightly reduced. In contrast, three of the four histidine-to-alanine substitutions in Gc either completely abolished (mutant H857A) or strongly impaired infectivity (mutants H778A and H1087A) to less than 5% relative to that of wild-type $RVFV_{ns}$.

H857 is essential for acid-induced rearrangement of Gc into higher order structures

Next we analyzed the effects of the histidine-to-alanine mutations on the formation, stability and conversion kinetics of the Gc oligomer. Acid exposure of similar amounts of mutant and wildtype $RVFV_{ns}$ particles resulted in the formation of the SDS-resistant Gc oligomer in all mutants, with the exception of mutant H857A (Fig. 6A, upper left panel). The Gc oligomers of mutants H778A, H836A and H1087A were not stable at 80°C in contrast to wildtype and the Gn histidine mutants (Fig. 6A, lower left panel). To analyze their thermostability in more detail, the Gc oligomers were subjected to heating at different temperatures prior to Western blot analysis. Compared to wildtype, the Gc oligomer of the H778A, H836A and H1087A mutants appeared slightly less thermostable and dissociated at 80°C but not at 70°C (Fig. 6A, right panels). Next, we assessed the effects of the mutations on the Gc conversion kinetics into the SDS-stable oligomer upon acid exposure, by Western blotting (Fig. 6B). Conversion kinetics of the Gc mutants H778A, H836A and H1087A upon pH treatment appeared grossly similar to that of wildtype (Fig. 6B). Clearly, acid exposure even up to 30 minutes of the Gc mutant carrying the lethal H857A substitution did not allow the formation of the SDS-resistant Gc oligomer (Fig. 6B) suggesting that the formation of the stable Gc oligomer induced by protonation of histidine 857, is essential for virus entry into the host cell. Finally, to assess a

possible shift in the pH activation threshold, we analyzed the Gc conversion for the H857A Gc mutant and wildtype $RVFV_{ns}$ particles at pH values below pH 5.5. Incubation at these acidic conditions for 10 minutes at 37ºC resulted in the formation of the stable oligomer in wildtype $RVFV_{ns}$ particles. In contrast, no stable Gc oligomer was observed after treatment of $RVFV_{ns}$ particles containing the H857A mutation (Fig. 6C).

Discussion

It is well established that bunyaviruses require the acidic pH found in endosomes to activate fusion, but it remains unclear how fusion is mediated at the molecular level. In this study we demonstrate that exposure of RVFV particles to acidic pH converts the viral Gc protein into a highly stable oligomer. The pH required for this major conformational change correlates with the pH threshold required to activate fusion of virus particles at the plasma membrane. Mutagenesis of conserved histidines in the viral glycoproteins identified a single histidine in Gc that was strictly required for entry as well as for the acid-induced conversion of Gc into its stable oligomeric form. These data provide new insight into the molecular basis of bunyavirus acid-activated fusion.

Most bunyaviruses studied to date utilize clathrin mediated endocytosis to gain access to the cell interior (22, 25, 38, 39, 55, 58). For UUKV a clathrin-independent pathway has been suggested as an alternative route (39). We demonstrate here that RVFV entry is sensitive to drugs perturbing the function of clathrin and dynamin, which is consistent with entry via a clathrin-mediated endocytic pathway. Further studies are required to confirm this assumption. Upon endocytosis, RVFV particles are transported deep into the cell through maturing endosomes. The pH threshold (pH<6) required for virus fusion at the plasma membrane and rearrangement of Gc suggests that fusion of RVFV occurs in late endosomes. This late penetration is consistent with the half-time of RVFV of ~20 minutes during which the virus undergoes its acid-activating step. Similar pH thresholds and penetration kinetics have been observed for UUKV, another *Phlebovirus* (39). Our data indicate that RVFV can be classified as a late-penetrating virus (38).

Exposure to low pH converts the $RVFV_{ns}$ Gc protein from an apparently metastable to a highly stable oligomeric conformation. Similar pH-induced rearrangements have been reported for envelope glycoproteins of other bunyaviruses. These conformational changes have been shown to either lead to dissociation of the Gn-Gc heterodimer (Hantavirus), to changes in the Gc antigenic structure or to

alteration in the cleavage pattern after proteolytic processing of the Gc protein (UUKV, La Crosse) (16, 21, 52). The low pH-induced changes in the glycoprotein shell of UUKV virions have been visualized nicely by electron microscopy, revealing the flattening of the glycoprotein capsomers (44, 52). Low pH incubation of La Crosse virus and UUKV leads to virus aggregation (44, 66). Activation of fusion proteins generally triggers the exposure of a hydrophobic 'fusion peptide' which normally functions by inserting into the host membrane and initiating fusion which might explain the observed acid-induced virus aggregation. Typically, fusion proteins are trimeric in this fusion active state (8, 17). Hence we assume that the RVFV Gc stable oligomer is also made up of three Gc molecules, but further research is needed to confirm this hypothesis.

The acid-induced Gc oligomer displays a remarkable resistance to temperature dissociation and SDS-detergent denaturation (10). In agreement with these observations back-neutralization of the acid-exposed virus particles did not reverse the transition of Gc into a stable oligomer. In general, viral fusion proteins convert to a stable form during fusion thereby generating the energy needed for membrane coalescence. For class I and II viral fusion proteins this transition was shown to be irreversible (51). Intriguingly, exposure of virus to the activating pH in the absence of target membranes also fully converts Gc into the stable oligomer; yet, although a reduction is seen, it does not completely inactivate virus infectivity, not even after incubation times of up to 16 minutes (data not shown). It remains to be seen whether the stable Gc oligomer represents the final post-fusion form of the Gc fusion protein or represents a crucial intermediate which awaits further reorganization. In the latter situation alternative factors (e.g. interaction with the target membrane) may be required to drive the conformational rearrangements to completion.

In the RVFV virion, Gc is organized as a heterodimer together with Gn (24). The Gn-Gc heterodimer is the building block of 110 hexamers and 12 pentamers containing six and five of the Gn-Gc heterodimeric units, respectively. Together these 122 capsomers make up the icosahedral shell of the virion following a T=12 triangulation (13, 24). Exposure of virions to the activating pH will lead to rearrangement of the metastable Gn-Gc heterodimer and concomitantly enforces the interactions between Gc subunits resulting in the formation of a Gc homo-oligomer. Exposure of virions to the acidic pH of 6 did not have any impact on the structure of RVFV particles, as shown by cryo-electron tomography, consistent with the fusion activating pH threshold of below 6 that we observed (24). It will be interesting to investigate how the Gc protomers in the virions - organized as pentamers and

hexameric Gn-Gc heterodimers - collectively undergo the structural transition towards the (presumably) trimeric Gc oligomer after exposure to the activating pH.

Protonation of histidines in Gc may play a key role at different stages of the fusion process. The inability of the H857A mutant to form stable Gc oligomers in combination with its abrogated entry function suggests that Gc oligomerization is essential for virus entry and that protonation of H857 plays a crucial role in this process. In addition, the substitution of H778 and H1087 in Gc has a severe effect on virus entry, yet Gc oligomerization still occurred and the temperature stability was only marginally affected. This suggests that formation of the Gc oligomer, although required, may not be sufficient for inducing fusion. We speculate that the single mutations may impair a later step in the fusion reaction (36). The H778, H857 and H1087 histidines in Gc may collectively contribute to pH sensing, initiation and propagation of conformational rearrangements towards the post-fusion structure. Further interpretation of the consequences of the histidine substitutions awaits the elucidation of the high-resolution structures of the Gc protein in its pre- and postfusion state.

Acknowledgement

We thank Rianka Vloet (Central Veterinary Institute, Lelystad) for assistance. We thank Dr. Christiaan Potgieter (ARC-OVI) for providing the 841 antiserum. We thank Dr. Sean Whelan and Dr. Matthijs Raaben (Harvard Medical School, Boston) for providing the VSVΔG-GFP recombinant virus. We thank Dr. Connie Schmaljohn (USAMRIID, Fort Detrick, Maryland, USA) for providing the 4-D4 monoclonal antibody recognizing Gn. This work was supported by the Dutch Ministry of Economic Affairs, Agriculture and Innovation, Project code KB-12-004.02-002.

References

1. **Arikawa, J., I. Takashima, and N. Hashimoto.** 1985. Cell fusion by haemorrhagic fever with renal syndrome (HFRS) viruses and its application for titration of virus infectivity and neutralizing antibody. Arch Virol **86:**303-313.
2. **Balkhy, H. H., and Z. A. Memish.** 2003. Rift Valley fever: an uninvited zoonosis in the Arabian peninsula. Int J Antimicrob Agents **21:**153-157.
3. **Boo, I., K. teWierik, F. Douam, D. Lavillette, P. Poumbourios, and H. E. Drummer.** 2012. Distinct roles in folding, CD81 receptor binding and viral entry for conserved histidine residues of hepatitis C virus glycoprotein E1 and E2. The Biochemical journal **443:**85-94.
4. **Carneiro, F. A., F. Stauffer, C. S. Lima, M. A. Juliano, L. Juliano, and A. T. Da Poian.** 2003. Membrane fusion induced by vesicular stomatitis virus depends on histidine protonation. J Biol Chem **278:**13789-13794.
5. **Chandran, K., N. J. Sullivan, U. Felbor, S. P. Whelan, and J. M. Cunningham.** 2005. Endosomal proteolysis of the Ebola virus glycoprotein is necessary for infection. Science **308:**1643-1645.
6. **Chanel-Vos, C., and M. Kielian.** 2006. Second-site revertants of a Semliki Forest virus fusion-block mutation reveal the dynamics of a class II membrane fusion protein. J Virol **80:**6115-6122.
7. **Chang, L. H., and M. F. Tam.** 1993. Site-directed mutagenesis and chemical modification of histidine residues on an alpha-class chick liver glutathione S-transferase CL 3-3. Histidines are not needed for the activity of the enzyme and diethylpyrocarbonate modifies both histidine and lysine residues. European journal of biochemistry / FEBS **211:**805-811.
8. **Cosset, F. L., and D. Lavillette.** 2011. Cell entry of enveloped viruses. Advances in genetics **73:**121-183.
9. **de Boer, S. M., J. Kortekaas, A. F. Antonis, J. Kant, J. L. van Oploo, P. J. Rottier, R. J. Moormann, and B. J. Bosch.** Rift Valley fever virus subunit vaccines confer complete protection against a lethal virus challenge. Vaccine **28:**2330-2339.
10. **Fass, D.** 2003. Conformational changes in enveloped virus surface proteins during cell entry. Advances in protein chemistry **64:**325-362.
11. **Filone, C. M., M. Heise, R. W. Doms, and A. Bertolotti-Ciarlet.** 2006. Development and characterization of a Rift Valley fever virus cell-cell fusion assay using alphavirus replicon vectors. Virology **356:**155-164.
12. **Findlay, G. M., and R. Daubney.** 1931. Rift Valley Fever. The lancet **218:**1350, 1367-1368.
13. **Freiberg, A. N., M. B. Sherman, M. C. Morais, M. R. Holbrook, and S. J. Watowich.** 2008. Three-dimensional organization of Rift Valley fever virus revealed by cryoelectron tomography. J Virol **82:**10341-10348.
14. **Fritz, R., K. Stiasny, and F. X. Heinz.** 2008. Identification of specific histidines as pH sensors in flavivirus membrane fusion. The Journal of cell biology **183:**353-361.
15. **Garry, C. E., and R. F. Garry.** 2004. Proteomics computational analyses suggest that the carboxyl terminal glycoproteins of Bunyaviruses are class II viral fusion protein (beta-penetrenes). Theoretical biology & medical modelling **1:**10.
16. **Gonzalez-Scarano, F.** 1985. La Crosse virus G1 glycoprotein undergoes a conformational change at the pH of fusion. Virology **140:**209-216.
17. **Harrison, S. C.** 2008. Viral membrane fusion. Nature structural & molecular biology **15:**690-698.
18. **Hartley, D. M., J. L. Rinderknecht, T. L. Nipp, N. P. Clarke, G. D. Snowder, A. National Center for Foreign, and F. Zoonotic Disease Defense Advisory Group on Rift Valley.** 2011. Potential effects of Rift Valley fever in the United States. Emerg Infect Dis **17:**e1.
19. **Helenius, A., J. Kartenbeck, K. Simons, and E. Fries.** 1980. On the entry of Semliki forest virus into BHK-21 cells. The Journal of cell biology **84:**404-420.
20. **Hepojoki, J., T. Strandin, H. Lankinen, and A. Vaheri.** 2012. Hantavirus structure - molecular interactions behind the scene. J Gen Virol.
21. **Hepojoki, J., T. Strandin, A. Vaheri, and H. Lankinen.** 2010. Interactions and oligomerization of hantavirus glycoproteins. J Virol **84:**227-242.
22. **Hollidge, B. S., N. B. Nedelsky, M. V. Salzano, J. W. Fraser, F. Gonzalez-Scarano, and S. S. Soldan.** 2012. Orthobunyavirus entry into neurons and other mammalian cells occurs via clathrin-mediated endocytosis and requires trafficking into early endosomes. J Virol.
23. **Howes, M. T., M. Kirkham, J. Riches, K. Cortese, P. J. Walser, F. Simpson, M. M. Hill, A. Jones, R. Lundmark, M. R. Lindsay, D. J. Hernandez-Deviez, G. Hadzic, A. McCluskey, R. Bashir, L. Liu, P. Pilch, H. McMahon, P. J. Robinson, J. F. Hancock, S. Mayor, and R. G. Parton.** 2010. Clathrin-independent carriers form a high capacity endocytic sorting system at the leading edge of migrating cells. The Journal of cell biology **190:**675-691.
24. **Huiskonen, J. T., A. K. Overby, F. Weber, and K. Grunewald.** 2009. Electron cryo-microscopy and single-particle averaging of Rift Valley fever virus: evidence for GN-GC glycoprotein heterodimers. J Virol **83:**3762-3769.
25. **Jin, M., J. Park, S. Lee, B. Park, J. Shin, K. J. Song, T. I. Ahn, S. Y. Hwang, B. Y. Ahn, and K. Ahn.** 2002. Hantaan virus enters cells by clathrin-dependent receptor-mediated endocytosis. Virology **294:**60-69.
26. **Kadlec, J., S. Loureiro, N. G. Abrescia, D. I. Stuart, and I. M. Jones.** 2008. The postfusion structure of baculovirus gp64 supports a unified view of viral fusion machines. Nature structural & molecular biology **15:**1024-1030.
27. **Kakach, L. T., T. L. Wasmoen, and M. S. Collett.** 1988. Rift Valley fever virus M segment: use of recombinant vaccinia viruses to study Phlebovirus gene expression. J Virol **62:**826-833.
28. **Kampmann, T., D. S. Mueller, A. E. Mark, P. R. Young, and B. Kobe.** 2006. The Role of histidine residues in low-pH-mediated viral membrane fusion. Structure **14:**1481-1487.
29. **Keegan, K., and M. S. Collett.** 1986. Use of bacterial expression cloning to define the amino acid sequences of antigenic determinants on the G2 glycoprotein of Rift Valley fever virus. J Virol **58:**263-270.
30. **Kielian, M.** 2006. Class II virus membrane fusion proteins. Virology **344:**38-47.
31. **Kielian, M., and F. A. Rey.** 2006. Virus membrane-fusion proteins: more than one way to make a hairpin. Nature reviews. Microbiology **4:**67-76.
32. **Kortekaas, J., A. Dekker, S. M. de Boer, K. Weerdmeester, R. P. Vloet, A. A. de Wit, B. P. Peeters, and R. J. Moormann.** 2010. Intramuscular inoculation of calves with an experimental Newcastle disease virus-based vector vaccine elicits neutralizing antibodies against Rift Valley fever virus. Vaccine **28:**2271-2276.
33. **Kortekaas, J., N. Oreshkova, V. Cobos-Jimenez, R. P. Vloet, C. A. Potgieter, and R. J. Moormann.** 2011. Creation of a nonspreading Rift Valley fever virus. J Virol **85:**12622-12630.

34. **Krishnan, A., S. K. Verma, P. Mani, R. Gupta, S. Kundu, and D. P. Sarkar.** 2009. A histidine switch in hemagglutinin-neuraminidase triggers paramyxovirus-cell membrane fusion. J Virol **83:**1727-1741.
35. **Le Blanc, I., P. P. Luyet, V. Pons, C. Ferguson, N. Emans, A. Petiot, N. Mayran, N. Demaurex, J. Faure, R. Sadoul, R. G. Parton, and J. Gruenberg.** 2005. Endosome-to-cytosol transport of viral nucleocapsids. Nature cell biology **7:**653-664.
36. **Li, Z., and G. W. Blissard.** 2011. Autographa californica multiple nucleopolyhedrovirus GP64 protein: roles of histidine residues in triggering membrane fusion and fusion pore expansion. J Virol **85:**12492-12504.
37. **Liu, L., C. C. Celma, and P. Roy.** 2008. Rift Valley fever virus structural proteins: expression, characterization and assembly of recombinant proteins. Virol J **5:**82.
38. **Lozach, P. Y., J. Huotari, and A. Helenius.** 2011. Late-penetrating viruses. Current opinion in virology **1:**35-43.
39. **Lozach, P. Y., R. Mancini, D. Bitto, R. Meier, L. Oestereich, A. K. Overby, R. F. Pettersson, and A. Helenius.** 2010. Entry of bunyaviruses into mammalian cells. Cell host & microbe **7:**488-499.
40. **Martin, K., and A. Helenius.** 1991. Transport of incoming influenza virus nucleocapsids into the nucleus. J Virol **65:**232-244.
41. **Mundel, B., and J. Gear.** 1951. Rift valley fever; I. The occurrence of human cases in Johannesburg. S Afr Med J **25:**797-800.
42. **Ogino, M., K. Yoshimatsu, H. Ebihara, K. Araki, B. H. Lee, M. Okumura, and J. Arikawa.** 2004. Cell fusion activities of Hantaan virus envelope glycoproteins. J Virol **78:**10776-10782.
43. **Ohkuma, S., and B. Poole.** 1978. Fluorescence probe measurement of the intralysosomal pH in living cells and the perturbation of pH by various agents. Proc Natl Acad Sci U S A **75:**3327-3331.
44. **Overby, A. K., R. F. Pettersson, K. Grunewald, and J. T. Huiskonen.** 2008. Insights into bunyavirus architecture from electron cryotomography of Uukuniemi virus. Proc Natl Acad Sci U S A **105:**2375-2379.
45. **Overby, A. K., R. F. Pettersson, and E. P. Neve.** 2007. The glycoprotein cytoplasmic tail of Uukuniemi virus (Bunyaviridae) interacts with ribonucleoproteins and is critical for genome packaging. J Virol **81:**3198-3205.
46. **Pepin, M., M. Bouloy, B. H. Bird, A. Kemp, and J. Paweska.** 2010. Rift Valley fever virus(Bunyaviridae: Phlebovirus): an update on pathogenesis, molecular epidemiology, vectors, diagnostics and prevention. Vet Res **41:**61.
47. **Piper, M. E., D. R. Sorenson, and S. R. Gerrard.** 2011. Efficient cellular release of Rift Valley fever virus requires genomic RNA. PLoS One **6:**e18070.
48. **Plassmeyer, M. L., S. S. Soldan, K. M. Stachelek, S. M. Roth, J. Martin-Garcia, and F. Gonzalez-Scarano.** 2007. Mutagenesis of the La Crosse Virus glycoprotein supports a role for Gc (1066-1087) as the fusion peptide. Virology **358:**273-282.
49. **Qin, Z. L., Y. Zheng, and M. Kielian.** 2009. Role of conserved histidine residues in the low-pH dependence of the Semliki Forest virus fusion protein. J Virol **83:**4670-4677.
50. **Rich, K. M., and F. Wanyoike.** 2010. An assessment of the regional and national socio-economic impacts of the 2007 Rift Valley fever outbreak in Kenya. Am J Trop Med Hyg **83:**52-57.
51. **Roche, S., A. A. Albertini, J. Lepault, S. Bressanelli, and Y. Gaudin.** 2008. Structures of vesicular stomatitis virus glycoprotein: membrane fusion revisited. Cellular and molecular life sciences : CMLS **65:**1716-1728.
52. **Ronka, H., P. Hilden, C. H. Von Bonsdorff, and E. Kuismanen.** 1995. Homodimeric association of the spike glycoproteins G1 and G2 of Uukuniemi virus. Virology **211:**241-250.
53. **Rusu, M., R. Bonneau, M. R. Holbrook, S. J. Watowich, S. Birmanns, W. Wriggers, and A. N. Freiberg.** 2012. An assembly model of rift valley Fever virus. Frontiers in microbiology **3:**254.
54. **Sanchez-San Martin, C., C. Y. Liu, and M. Kielian.** 2009. Dealing with low pH: entry and exit of alphaviruses and flaviviruses. Trends in microbiology **17:**514-521.
55. **Santos, R. I., A. H. Rodrigues, M. L. Silva, R. A. Mortara, M. A. Rossi, M. C. Jamur, C. Oliver, and E. Arruda.** 2008. Oropouche virus entry into HeLa cells involves clathrin and requires endosomal acidification. Virus Res **138:**139-143.
56. **Schmaljohn, C. S., Nichol, S.T.** 2007. Bunyaviridae, p. 1741-1789. *In* D. M. Knipe, Howley, P.M. (ed.), Fields virology, 5th Edition, vol. 2. Lippincott williams & Wilkins.
57. **Schowalter, R. M., A. Chang, J. G. Robach, U. J. Buchholz, and R. E. Dutch.** 2009. Low-pH triggering of human metapneumovirus fusion: essential residues and importance in entry. J Virol **83:**1511-1522.
58. **Simon, M., C. Johansson, and A. Mirazimi.** 2009. Crimean-Congo hemorrhagic fever virus entry and replication is clathrin-, pH- and cholesterol-dependent. J Gen Virol **90:**210-215.
59. **Stiasny, K., S. L. Allison, A. Marchler-Bauer, C. Kunz, and F. X. Heinz.** 1996. Structural requirements for low-pH-induced rearrangements in the envelope glycoprotein of tick-borne encephalitis virus. J Virol **70:**8142-8147.
60. **Struthers, J. K., R. Swanepoel, and S. P. Shepherd.** 1984. Protein synthesis in Rift Valley fever virus-infected cells. Virology **134:**118-124.
61. **Thoennes, S., Z. N. Li, B. J. Lee, W. A. Langley, J. J. Skehel, R. J. Russell, and D. A. Steinhauer.** 2008. Analysis of residues near the fusion peptide in the influenza hemagglutinin structure for roles in triggering membrane fusion. Virology **370:**403-414.
62. **Tischler, N. D., A. Gonzalez, T. Perez-Acle, M. Rosemblatt, and P. D. Valenzuela.** 2005. Hantavirus Gc glycoprotein: evidence for a class II fusion protein. J Gen Virol **86:**2937-2947.
63. **Vaney, M. C., and F. A. Rey.** 2011. Class II enveloped viruses. Cellular microbiology **13:**1451-1459.
64. **Wahlberg, J. M., and H. Garoff.** 1992. Membrane fusion process of Semliki Forest virus. I: Low pH-induced rearrangement in spike protein quaternary structure precedes virus penetration into cells. The Journal of cell biology **116:**339-348.
65. **Walter, C. T., and J. N. Barr.** 2011. Recent advances in the molecular and cellular biology of bunyaviruses. J Gen Virol **92:**2467-2484.
66. **Wang, G. J., M. Hewlett, and W. Chiu.** 1991. Structural variation of La Crosse virions under different chemical and physical conditions. Virology **184:**455-459.
67. **Weissenhorn, W., A. Hinz, and Y. Gaudin.** 2007. Virus membrane fusion. FEBS letters **581:**2150-2155.
68. **White, J., K. Matlin, and A. Helenius.** 1981. Cell fusion by Semliki Forest, influenza, and vesicular stomatitis viruses. The Journal of cell biology **89:**674-679.
69. **Yoshimura, A., K. Kuroda, K. Kawasaki, S. Yamashina, T. Maeda, and S. Ohnishi.** 1982. Infectious cell entry mechanism of influenza virus. J Virol **43:**284-293.

584

585 FIG 1 Rift Valley fever virus enters the cell via endocytosis. (A) BHK-21 cells were pre-treated for 1
586 hour with two-fold dilutions of the indicated drugs and inoculated with $RVFV_{ns}$ (moi~0.1) or VSV_{ns}
587 (moi~0.8) for 2 hours in the continued presence of the drugs after which the inoculum was replaced by
588 culture medium containing bafilomycin A1 (10-40 nM) to inhibit further RVFV entry (see Fig.2).
589 Infection was quantified 20 hours ($RVFV_{ns}$) or 8 hours (VSV_{ns}) post infection by measuring GFP-
590 positive cells using FACS. The data are the means of three independent experiments done in
591 duplicate. ND; no drugs, SO; solvent (1% DMSO), dyn; dynasore, nys; nystatin, cyt; cytochalasin D,
592 chl; chlorpromazine. (B) BHK-21 cells were incubated with the indicated drugs for three hours after
593 which medium containing the drugs was replaced for culture medium containing bafilomycin A1 (20
594 nM). Twenty hours later, the effect of the chemical compounds on the metabolic activity of the cells
595 was determined using a spectrophotometric assay. Cells were considered viable if the relative
596 metabolic activity of treated cells remained above 70% (indicated by the dashed line) relative to
597 untreated cells (ND). The results shown are representative of two independent experiments performed
598 in triplicate. dgo; dyngo-4a. (C) BHK-21 cells were infected with $RVFV_{ns}$ (moi~0.2) for 2 hours after
599 which infection was continued for three hours in the presence of 80 or 40 μM dynasore or 20 or 40 μM
600 chlorpromazine. Cells were incubated overnight in culture medium containing bafilomycin A1 (20 nM).
601 At twenty hours post infection, infected (GFP-positive) cells were quantified by FACS. Data shown are
602 representative of two independent experiments performed in duplicate. NI; not infected. (D) Analysis of
603 the effect of dyngo-4a on $RVFV_{ns}$ and VSV_{ns} infection (moi ~0.4) of BHK-21 cells. Infection was
604 performed and quantified as described under (A). (E) Representative fluorescence pictures of BHK-21
605 cells infected with $RVFV_{ns}$ or $RVFV_{rec}$ in the presence of dynasore (80μM) or chlorpromazine (40μM).
606 Infection was performed as described under (A) at a moi of ~0.2. Nuclei were stained with DAPI.
607 Pictures are representative of two independent experiments performed in duplicate.

608 Fig 2 Entry of $RVFV_{ns}$ depends on vacuolar acidification. (A) BHK-21 or A549 cells were pre-treated
609 for 1 hour with different concentrations of bafilomycin A1 or ammonium chloride (NH4Cl) and
610 subsequently infected with $RVFV_{ns}$ (moi~0.1) or VSV_{ns} (moi~0.8). Infection (GFP-positive cells) was
611 quantified by FACS. Results shown are representatives of three individual experiments performed in
612 duplicate. NI; not infected, ND; no drugs. (B) $RVFV_{ns}$ was bound to BHK-21 cells for 1 hour in the cold
613 and subsequently warmed to 37°C. NH4Cl (10mM) was added at indicated times to instantly raise the

endosomal pH thereby inhibiting further infection. Eighteen hours post warming, infection (GFP-positive cells) was analyzed by fluorescence microscopy and quantified by FACS. Untreated cells yielded ~70% infection. Graphical data shown are representative of two independent experiments performed in duplicate. NI; not infected, ND; no drugs, C; NH4Cl control (not infected).

FIG 3 Low pH-activated penetration of cell-bound $RVFV_{ns}$ and inactivation of unbound $RVFV_{ns}$ particles. (A) $RVFV_{ns}$ was allowed to bind in the cold to a confluent monolayer of BHK-21 cells for 2 h before the cell-bound virus was exposed for 3 minutes at 37°C at the indicated pH. Infection was continued in culture medium containing bafilomycin A1 (20 nM) to inhibit infection via the endocytic route. Infection (GFP-positive cells) was analyzed 20 hours post warming by fluorescence microscopy and was quantified by FACS. Untreated cells (pH 7.4) yielded ~40% infection. The results shown are representative of two individual experiments performed in triplicate. (B) $RVFV_{ns}$ particles were incubated at the indicated pH for 3 minutes at 37°C. After neutralization of the medium infectivity of the virus was assayed on BHK-21 cells. Infection (GFP-positive cells) was analyzed 20 hours post infection by fluorescence microscopy and quantified by FACS. Virus incubated at neutral pH resulted in ~30% GFP positive cells. Graphical data shown are representative of four individual experiments performed in duplicate. The control in A and B represent cells that are not infected (NI).

FIG 4 Acid exposure triggers the formation of a SDS- and temperature-resistant Gc oligomer. (A) $RVFV_{ns}$ particles were exposed to the indicated pH for 10 minutes at 37ºC, returned to neutral pH and subsequently analyzed by Western blotting performed under non-reducing conditions. RVFV glycoproteins were detected with a RVFV serum, a monoclonal antibody against Gn or a polyclonal Gc peptide serum. In some cases Gc migrates as a closely spaced doublet. (B) $RVFV_{ns}$ particles were exposed for 10 minutes to pH 5.5 at 37ºC, returned to neutral pH and heated for 20 minutes at the indicated temperatures. Samples were subsequently analyzed by Western blotting (non-reducing conditions) using a RVFV serum or a Gc peptide serum. (C) $RVFV_{ns}$ particles were exposed to pH 5.5 at 37ºC for the indicated times and analyzed by Western blotting (non-reducing conditions) using a polyclonal serum raised against the purified Gc ectodomain (Gce). OC; oligomeric complex, NC; negative control (medium from mock-transfected replicon cells), RT; room temperature.

FIG 5 Role of histidines in $RVFV_{ns}$ infectivity. (A) $RVFV_{ns}$ was pre-treated with different concentrations of DEPC for ten minutes at 37ºC and subsequently assayed for infectivity. Infectivity (GFP-positive cells) was analyzed 20 hours post inoculation by fluorescence microscopy and quantified by FACS.

644 BHK-21 cells inoculated with 0μM DEPC treated virus yielded ~20% infection. Graphical data shown
645 are representative of two independent experiments performed in triplicate. SC; solvent control (0.2%
646 ethanol). (B) Membrane topology of the RVFV M-segment encoding polyprotein starting from the
647 fourth methionine (adapted from (16)). The predicted N-linked glycosylation sites (Y symbols) and
648 signal peptidase cleavage sites (scissors) are indicated. The luminal domain of Gn and Gc and the
649 cytoplasmic domains of Gn and Gc are colored in blue, green, grey and pink, respectively. The orange
650 blocks represent the transmembrane spanning regions. The position and amino acid numbering of
651 conserved histidines (H), calculated from the first methionine (JF784387), are indicated in the linear
652 diagram of the GnGc polyprotein. (C) Equal amounts of wildtype and mutant $RVFV_{ns}$ containing
653 histidine-to-alanine substitutions determined by a dot blot assay (two-fold dilutions of viruses are
654 shown) were analyzed for their infectivity on BHK-21 cells. BHK-21 cells inoculated with wildtype
655 $RVFV_{ns}$ particles resulted in ~20% infection. Infection (GFP-positive cells) was quantified by FACS.
656 Non-infected (NI) BHK-21 cells were included as a negative control. The data shown represent the
657 combined results of three independently produced batches of wildtype and mutant $RVFV_{ns}$ particles
658 tested in independent experiments, each performed in triplicate.

659 FIG 6 Effects of histidine substitutions in RVFV glycoproteins on the formation and stability of the Gc
660 oligomer. (A) Equal amounts of wildtype and mutant $RVFV_{ns}$ particles were exposed for 10 minutes to
661 pH 5.5 at 37ºC, returned to neutral pH, heated for 20 minutes at the indicated temperatures and
662 subsequently analyzed by Western blotting (non-reducing conditions) using a polyclonal serum raised
663 against the Gc ectodomain (Gce). In some cases Gc runs as a closely spaced doublet. The
664 thermostability of the acid-induced Gc oligomer is indicated for the wildtype and Gn- and Gc-His
665 mutant $RVFV_{ns}$ particles at 20°C and 80°C (left panel) or for the wildtype and the Gc-His mutant
666 $RVFV_{ns}$ particles at 40°C, 70°C and 80°C (right panel). (B) Equal amounts of wildtype and mutant
667 $RVFV_{ns}$ particles containing histidine-to-alanine mutations in Gc were exposed to pH 5.5 at 37ºC for
668 the indicated times and analyzed by Western blotting (non-reducing conditions) using a polyclonal
669 serum raised against the Gc ectodomain. OC represents the oligomeric complex, WT; wildtype. (C)
670 Equal amounts of wildtype and H857A mutant $RVFV_{ns}$ particles were exposed for 10 minutes at 37ºC
671 at the indicated pH. The Gc conversion was analyzed by Western blotting as described under B.

Table 1. Conservation of the selected histidines in the RVFV Gn and Gc glycoproteins among members of the *Phlebovirus* genus of the *Bunyaviridae* family as determined by ClustalW alignment.

***Phlebovirus* Strains (GenBank accession number)**	**Gn protein**				**Gc protein**			
	AA157*	AA540	AA572	AA580	AA778	AA836	AA857	AA1087
RVFV (JF784387)	H	H	H	H	H	H	H	H
SFNV (YP089671)	H	H	H	H	H	H	H	H
TOSV (AB385175)	H	H	H	H	H	H	H	H
MASV (AC1240II)	H	H	H	H	H	H	H	H
Echarte virus (HM119411)	H	Y	Y	H	H	H	H	H
TUAV (HM119432)	H	H	N	H	H	H	H	H
CDUV (HM119408)	H	H	N	H	H	H	H	H
MCRV (HM119420)	H	H	Q	H	H	H	H	H
ARQV (HM119405)	H	H	S	H	H	H	H	H
MRMBV (HM119423)	H	H	T	H	H	H	H	H
ALEV (HM119414)	H	H	K	H	H	H	H	H
ITAV (HM119417)	H	H	K	H	H	H	H	H
SRNV (HM119429)	H	Y	K	H	H	H	H	H
NIQV (HM119426)	H	H	N	H	H	H	H	H
ORXV (HM119435)	H	Y	H	H	H	H	H	H
JCNV (HM466935)	H	Y	Y	H	H	H	H	H
SFSV (AAA75043	H	H	E	H	R	H	H	H
PTV (ABD92923)	H	H	H	H	H	H	H	H
SFTSV (HM745931)	- **	H	E	Y	R	R	P	S
UUKV (AAA79512)	- **	R	A	F	H	R	Y	H

* Amino acid (AA) numbers correspond to the RVFV M-segment encoding polyprotein.

** ClustalW alignment displays a gap at this position

Fig. 1

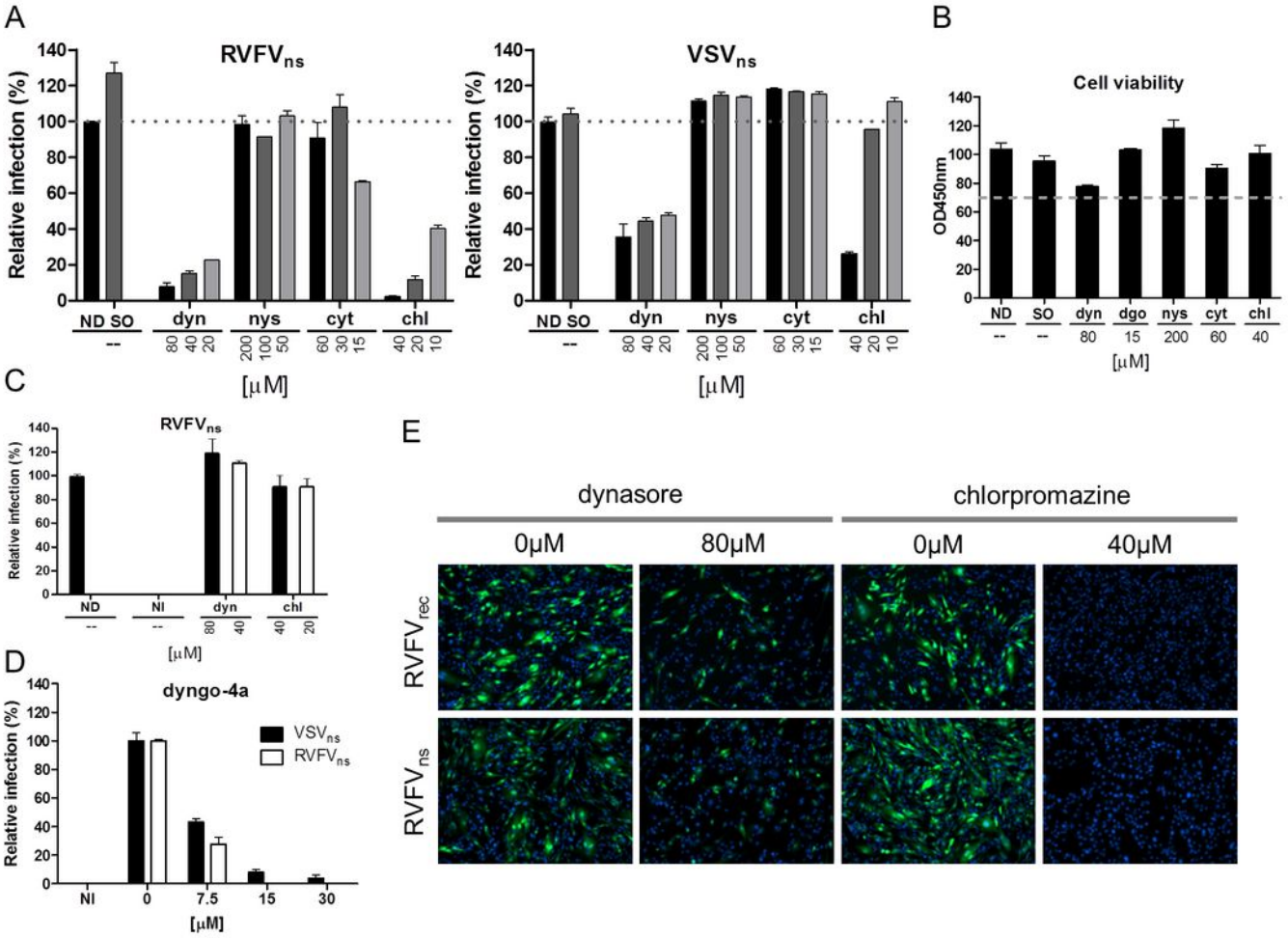

Fig. 2

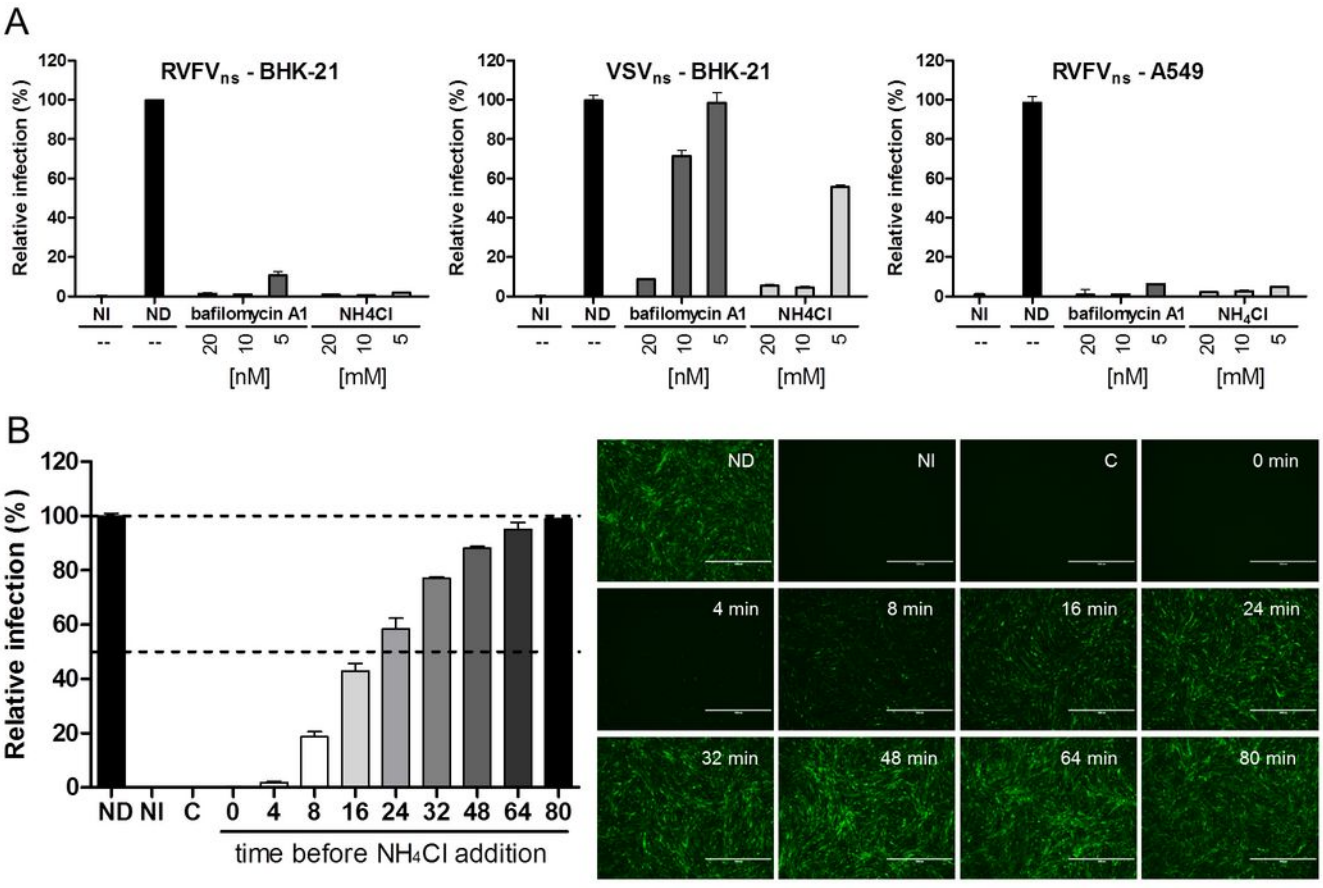

Fig. 3

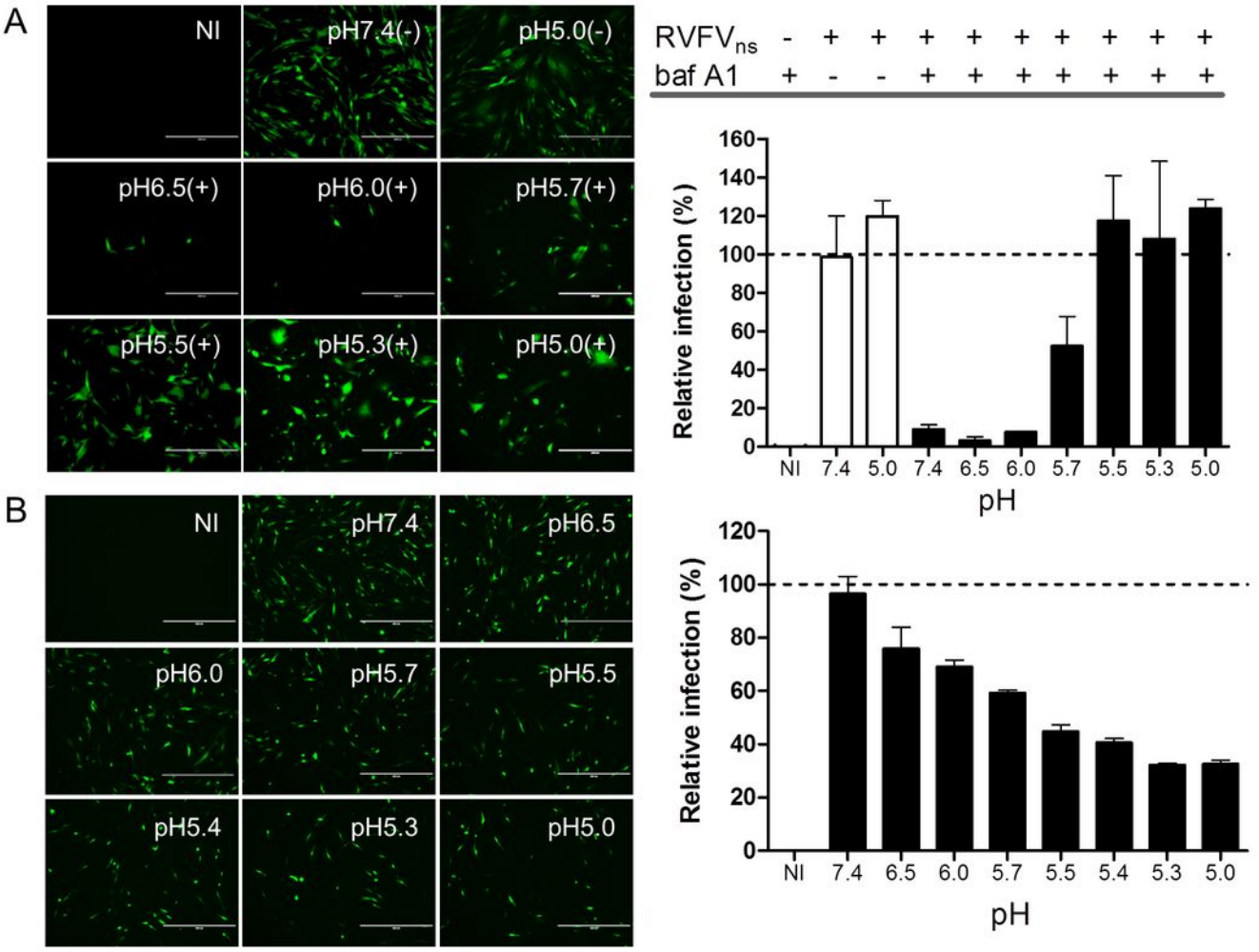

Fig. 4

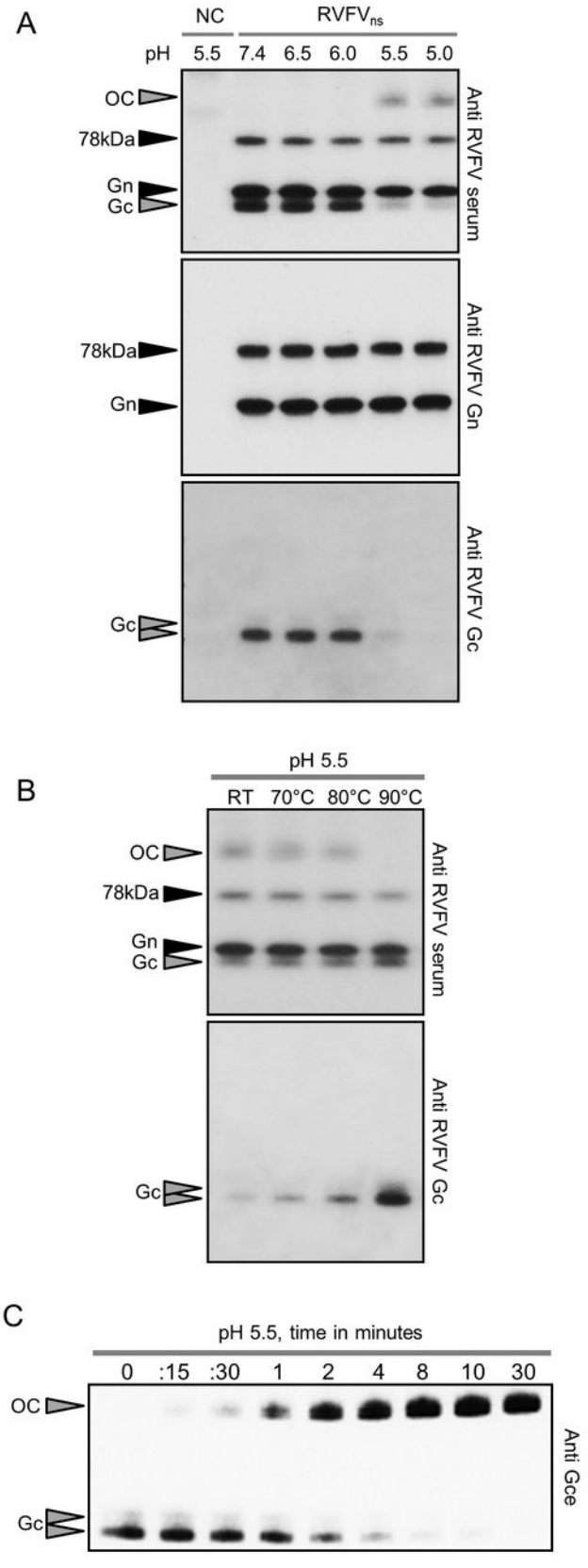

Fig. 5

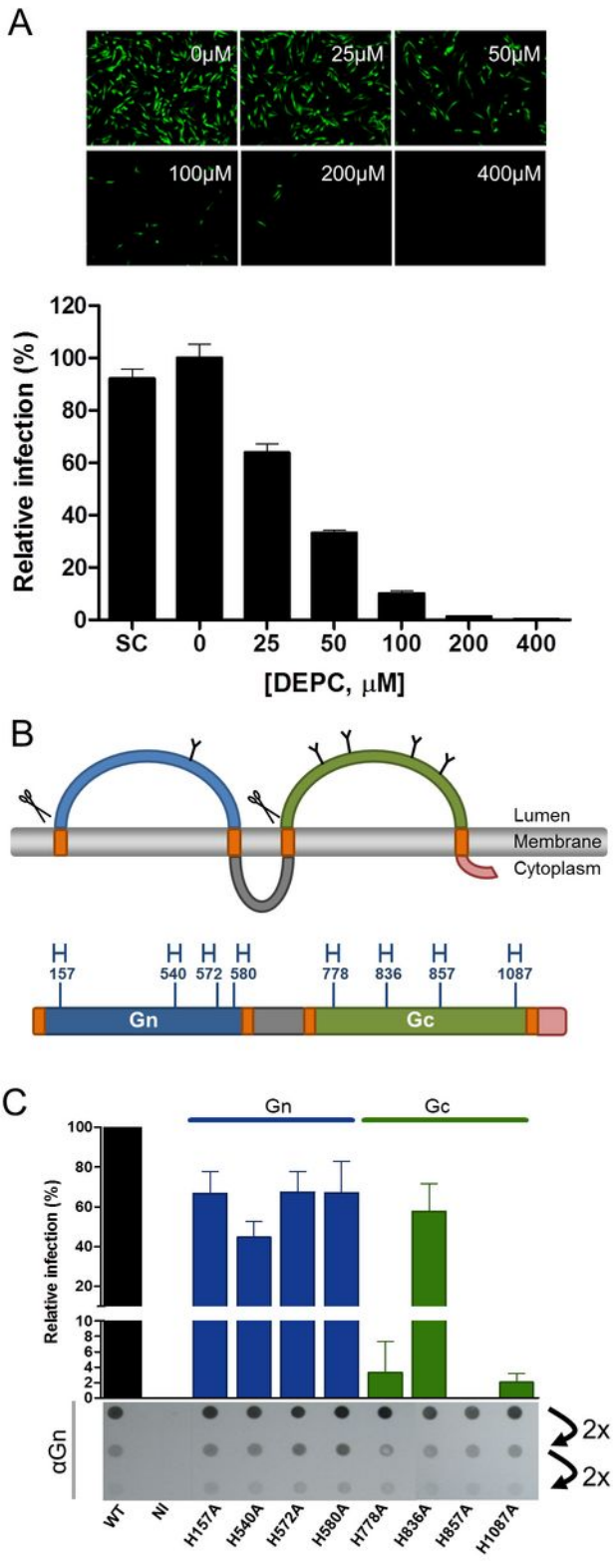

Fig. 6